Hindawi
Advances in Civil Engineering
Volume 2020, Article ID 3534957, 14 pages
https://doi.org/10.1155/2020/3534957

Research Article

Damaged Flexibility Matrix Method for Damage Detection of Frame Buildings

Luis S. Vaca Oyola,[1] **Mónica R. Jaime Fonseca**,[1] **and Ramsés Rodríguez Rocha**[2]

[1]*Centro de Investigación en Ciencia Aplicada y Tecnología Avanzada Unidad Legaria, IPN. Av. Legaria 694, Col. Irrigación, Ciudad de Mexico 11500, Mexico*
[2]*Department of Structural Engineering, Escuela Superior de Ingeniería y Arquitectura, IPN, Av. Juan de Dios Batiz, Edificio de Posgrado, Col. Zacatenco, Ciudad de Mexico 07738, Mexico*

Correspondence should be addressed to Luis S. Vaca Oyola; lvacao1300@alumno.ipn.mx

Received 2 October 2019; Revised 2 January 2020; Accepted 7 January 2020; Published 10 February 2020

Academic Editor: Filippo Ubertini

This study presents the damaged flexibility matrix method (DFM) to identify and determine the magnitude of damage in structural elements of plane frame buildings. Damage is expressed as the increment in flexibility along the damaged structural element. This method uses a new approach to assemble the flexibility matrix of the structure through an iterative process, and it adjusts the eigenvalues of the damaged flexibility matrices of each system element. The DFM was calibrated using numerical models of plane frames of buildings studied by other authors. The advantage of the DFM, with respect to other flexibility-based methods, is that DFM minimizes the adverse effect of modal truncation. The DFM demonstrated excellent accuracy with complete modal information, even when it was applied to a more realistic scenario, considering frequencies and modal shapes measured from the recorded accelerations of buildings stories. The DFM also presents a new approach to simulate the effects of noise by perturbing matrices of flexibilities. This approach can be useful for research on realistic damage detection. The combined effects of incomplete modal information and noise were studied in a ten-story four-bay building model taken from the literature. The ability of the DFM to assess structural damage was corroborated. Application of the proposed method to a ten-story four-bay building model demonstrates its efficiency to identify the flexibility increment in damaged structural elements.

1. Introduction

The dynamics of our planet require that existing buildings withstand increasingly complex combinations of loads, such as earthquakes and intense winds. It is inevitable that construction materials age, experience temperature changes, and suffer chemical reactions due to the environmental conditions. All these factors cause damage to buildings during their useful life, especially in areas of high seismicity such as Mexico, where earthquakes have caused serious damage [1–3]. In September 2017, earthquakes caused critical damage to buildings in Mexico City and in other smaller communities [4]. Knowing the location and extent of structural damage in a building can prevent its catastrophic collapse [5–10].

Assessing the structural health of a structure is important; it is thus necessary to define a damage index that allows monitoring the structural health of a building. In general, a damage index is defined as the change of a system characteristic that allows a quantitative comparison between the undamaged state and the damaged one. Some authors define the damage index as a loss of stiffness [11–13], as an increase of flexibility [14, 15], or as modal strain energy changes [16, 17], among other definitions [18–21].

In the literature, there are many experimental studies showing that frequencies and modal shapes may be suitable parameters for the diagnosis and monitoring of the structural health of a structure [22–25]. However, during the last decades, many researchers have been developing practical and efficient methods for the identification of structural

damage using dynamic properties of buildings. For example, Rodríguez et al. [26] presented a damage detection method called Damage Submatrices Method (DSM), which expresses the damage intensity as the loss of stiffness of a structural element. This method can identify damage in specific zones using the natural frequencies and modal shapes of the undamaged and damaged structure.

Fan and Qiao [18] presented an exhaustive review of damage identification methods based on modal parameter changes, as well as on the main damage identification algorithms of signal processing. They classified damage identification methods into four categories according to their vibration characteristics: methods based on natural frequencies, methods based on modal shapes, methods based on curvature shapes, and methods combining modal shapes and frequencies. They reported that most of the methods based on modal shapes and curvature shapes are more effective to locate the damage of a building. However, these methods are very sensitive to optimization algorithms or signal processing techniques. In this paper, we use a combined method of shapes and modal frequencies to adjust flexibility matrices of the structure. Using these matrices, the DFM identifies accurately damaged elements.

In the field of structural damage detection, application of the flexibility matrix of a structure has drawn the attention of many researchers, because of its high sensitivity for damage location, and because it can be accurately estimated using only a few modal shapes. These advantages have allowed the use of the flexibility matrix to develop various damage detection methods. Li et al. [27] developed a damage identification method using a "generalized flexibility matrix," by which they used to detect changes in stiffness in a simply supported beam using frequencies and modal shapes of the damaged and undamaged structure. Weng et al. [28] proposed a new substructuring method for damage detection in a structure; they obtained substructural flexibility matrices corresponding to each substructure and calculated the corresponding eigenvalues and eigenvectors to use them as indicators of damage. This method is very sensitive to localized damage; however, it is necessary to have many accelerometers close to the damage location. Katebi et al. [29] proposed a modified modal flexibility method, which is based on updating a proposed sensitivity equation derived from a finite element model. This method determines the modal flexibility that is used to detect and quantify the damage. However, because it requires numerous sensors, it is not practical to use it on experimental models. Bernagozzi et al. [30] developed a method for detecting damage in shear buildings when the mass of the system is not known or when there is very little information about it. This method estimates the modal deflections that are proportional to real deflections; after this estimation, the story drifts are evaluated to locate loss of stiffness. Bernagozzi's method only locates the damaged story and not each structural element damaged; thus, it can only be used if the acceleration records of all stories in a building are available.

Many damage detection methods based on structural flexibility have been developed. Despite their ability to estimate the flexibility matrix of a structure from measured lower-order modal shapes, these methods still suffer from modal truncation error, particularly on a complex structure with many higher modes that are not measured [27–30]. In this paper, we present the damaged flexibility matrix method (DFM), a new iterative damage detection method using the procedure developed by Baruch [31], to optimize and correct flexibility matrices from vibration measurements. In contrast to other methods, the DFM was highly accurate in the damage cases studied, when limited modal information was available, thus minimizing errors related to higher-order modal truncation. The DFM locates and evaluates the flexibility increase in any structural element of a plane frame of a building, based on the frequencies and modal shapes of damaged and undamaged structures. A damage index is defined representing the flexibility increase of each structural element. The DFM is based on eigenvalue decomposition. In contrast to the existing methods, the DFM assigns an individual indicator of damage to each structural element. The method was calibrated using numerical model of a ten-story four-bay building taken from the related literature. The DFM was validated by comparing it with the DSM, taking into account measurements of limited modal information. Finally, a new procedure was proposed, and it was used to simulate noise in modal measurements, perturbing flexibility matrices. Study cases corroborated the practicality and ability of the DFM to identify and assess the damage of structural elements of a building.

This article is organized as follows: Section 2 is dedicated to the theoretical background; a way to assemble the flexibility matrix of a plane frame, its application in structural damage detection, and the DFM algorithm are presented. In Section 3, the DFM was calibrated using a ten-story and four-bay frame building, then the DFM was applied to this frame building, which was damaged during the earthquake in Mexico on September 19, 1985 [32]. This building was previously studied by Escobar et al. using a structural damage detection method called Matrix Transformation Method [33], and by Rodríguez et al. using the Baseline Stiffness Method [34]. This building is representative of Mexico City; it is located in the lake area, according to its seismic zoning map [35]. In Section 4 the effects of limited modal information and noise are evaluated on our method. Finally, in Section 5 a more realistic scenario was studied, considering records of accelerations taken from the stories of the building, and the effects of noise.

2. DFM

The global flexibility matrix F of a plane frame without damage, with a number of general degrees of freedom (dof), can be expressed as (see Appendix A)

$$F = \sum_{i=1}^{N} [B]_i^T * [Fe]_i * [B]_i, \tag{1}$$

where $[B]i$ are equilibrium matrices representing the relationship between generalized loads and internal loads, whose order is $m \times \text{dof}$. The numbers of internal loads of each structural element are represented by m. The matrix

$[B]i$ is obtained by applying unit loads to each dof considered; then, the internal loads of each structural element are obtained. $[Fe]_i$ are the flexibility matrices of each structural element of the structure. Similar to other studies [26, 27, 33, 36], in our model the damaged global flexibility matrix $[F]_D$ of the structure can be calculated as the difference between the flexibility matrix of the undamaged structure $[F]$ and the contribution of flexibilities matrices $[Fe]_i$ corresponding to the i-th element multiplied by a scalar damage indicator $[x]_i$; that is,

$$[F]_D = [F] - \sum_{i=1}^{N} [x]_i * [B]_i^T * [Fe]_i * [B]_i, \tag{2}$$

where N is the total number of elements of the structure and x_i contains information about the flexibility increase of each damaged structural element in the form:

$$[x]_i = \begin{bmatrix} x_i & 0 & 0 \\ 0 & \ddots & 0 \\ 0 & 0 & x_i \end{bmatrix}. \tag{3}$$

The index x_i varies from 0 to 1; zero represents no damage and one represents completely damaged. It is important to note that this work does not intend to study the damage derived from the sudden removal of beams or columns. For this reason, the damage cases studied will involve a certain level of damage (increased flexibility) caused by changes in the properties of the material.

Substituting (1) into (2) and rewriting the equation, we get

$$[F] - [F]_D = [x]_1 * [B]_1^T * [Fe]_1 * [B]_1 + [x]_2 * [B]_2^T * [Fe]_2 * [B]_2 + \cdots + [x]_N * [B]_N^T * [Fe]_N * [B]_N. \tag{4}$$

Using matrix notation, this equation can be written as

$$[F] - [F]_D = \begin{bmatrix} x_1 & 0 & 0 \\ 0 & \ddots & 0 \\ 0 & 0 & x_1 \end{bmatrix} * [B]_1^T * [Fe]_1 * [B]_1 + \begin{bmatrix} x_2 & 0 & 0 \\ 0 & \ddots & 0 \\ 0 & 0 & x_2 \end{bmatrix} * [B]_2^T * [Fe]_2 * [B]_2 + \cdots + \begin{bmatrix} x_N & 0 & 0 \\ 0 & \ddots & 0 \\ 0 & 0 & x_N \end{bmatrix} * [B]_N^T * [Fe]_N * [B]_N. \tag{5}$$

Grouping all the matrices that contain the damage indicators x_i and rewriting the previous expression in a compact form, the following equation is obtained:

$$[F] - [F]_D = [X] * [F_s], \tag{6}$$

where the rectangular matrix $[X]$ is of size of dof $\times$ (dof $\times N$) and contains squared submatrices corresponding to each damage indicator x_i. Similarly, $[F_s]$ is of size (dof $\times N$) $\times$ dof and has the following form:

$$[F_s] = \left[[B]_1^T * [Fe]_1 * [B]_1, [B]_2^T * [Fe]_2 * [B]_2, \ldots, [B]_N^T * [Fe]_N * [B]_N \right]^T. \tag{7}$$

The objective of our damage detection method is to calculate the unknown matrix $[X]$ of equation (6), which can be achieved using the pseudoinverse method [37] applied to equation (7): $[F_s]^\dagger$. $[X]$ can thus be written as

$$[X] = \left[[F] - [F]_D \right] * [F_s]^\dagger, \tag{8}$$

where $[X]$ can be broken down into N square matrices $[x_s]_i$ containing information about the damage of each structural element. Grouping elements of matrix $[X]$,

$$[X] = \left[[x_s]_1 \; [x_s]_2 \; [x_s]_3 \ldots [x_s]_i \ldots [x_s]_N \right]. \tag{9}$$

Matrix damage indicators will be obtained from equation (9). However, a scalar indicator for each structural element is needed. One approach used by many researchers to describe a matrix that contains damage information is eigenvalue decomposition [11, 28, 34, 38, 39]. Applying this approach to each matrix $[x_s]_i$ we obtain

$$\left[[x_s]_i - \lambda * [I] \right] [\phi] = [0], \tag{10}$$

where λ and $[\phi]$ are a scalar eigenvalue and eigenvector of matrix $[x_s]_i$ and the matrix $[I]$ is a unit matrix. According the fundamental property of eigenvalue decomposition, after equation (10) is solved and after the eigenvector matrix $[\Phi]_i$ containing all the eigenvectors $[\phi]$ is obtained, the corresponding eigenvalue λ is stored in a diagonal squared matrix $[\Lambda]_i$; from this matrix, a single scalar value is taken as a damage indicator, whose greatest eigenvalue will be the scalar indicator of damage selected x_i^*. This scalar value yields lower levels of relative errors for a determined number of iterations, meaning that the detection method converges faster. Faster convergence was expected since the greatest eigen value from matrix $[x_s]_i$ is related to the energy level characterizing the system [37].

The objective of the DFM will be to obtain all the values x_i of each structural element, until a minimum tolerance e, between $[F]_D$ and the approximate damaged flexibility matrix $[F_D]_{\text{aprox}}$ is obtained. This is achieved through an iterative process, in which the damage indicator identified x_i^* in each iteration accumulates with the damage indicator obtained in the previous iteration; this new damage indicator x_i is substituted into equation (2) in order to obtain an approximate flexibility matrix $[F_D]$ for the next iteration. The following algorithm is proposed to identify damage in structural elements, based on flexibility matrices (see Appendix B for more details):

2.1. Ten-Story Four-Bay Plane Frame Building. In order to demonstrate the efficiency of the proposed method for damage identification using simulated damage in a complex structure, the DFM was applied to a ten-story and four-bay frame building belonging to the Mass Transportation System Authority of Mexico (thereafter

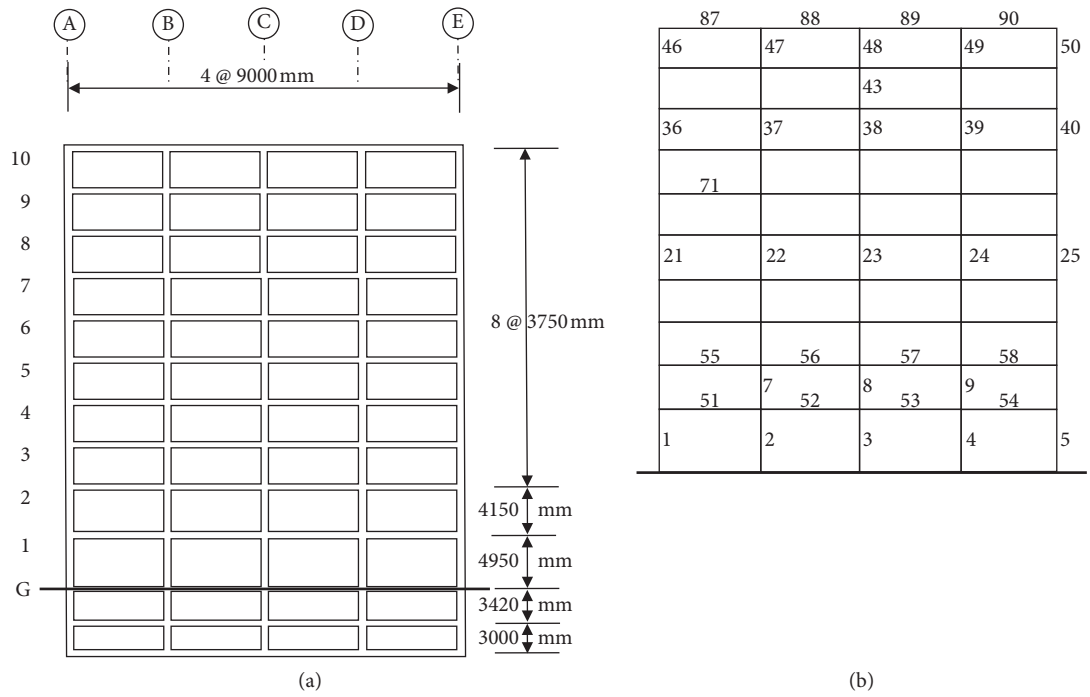

Figure 1: Ten-story four-bay MTSAM frame building model. (a) Geometry. (b) Structural elements.

MTSAM). This building is located in Mexico City (Figure 1); it has a regular geometry in plan with shear walls in the transverse direction; therefore seismic biaxial effects are minimal for the interior frame that we studied in this article. Figure 1(a) shows the building's elevation geometry. Figure 1(b) shows the numbering assigned to its structural elements. The cross-sections of all beams are 400×900 mm; columns along axes A and E on all stories are 500×900 mm; columns along B, C, and D axes of stories 1 and 2 are 500×900 mm; columns of stories 3 and 4 are 500×800 mm; columns of stories 5 and 6 are 500×700 mm; and columns of stories 7 to 10 are 500×600 mm. The weight of floors 1 to 9 is 1,451 kN and weight of floor 10 is 1,161 kN. Elastic modulus E is 14.7 GPa.

The first step to validate the DFM was to use complete modal information of the structure. Thus, we decided to study the damage cases D1, D2, and D3 that were analyzed by Rodríguez et al. [26]. Table 1 compares our results with those reported by Rodriguez et al. It should be noted that the damage was simulated by changing the section properties of structural elements, which resulted in a flexibility increase along the length of the damaged structural element. Therefore, when we compared the relative errors of the DSM and the DFM (Table 1), we were comparing the ability of both methods to detect and identify damage in structural elements at specific locations. The damage cases analyzed represent an irregular distribution of the damage. The damage case D1 includes damaged structural elements located at different stories. Cases D2 and D3 include damage located on the first and last stories, respectively. It is important to note that the distribution of damage that we selected intends to simulate the distribution of the real damage corresponding to what was observed by visual inspection after the earthquake.

According to the results shown in Table 1 for the three damage cases analyzed (D1–D3), the DFM identified all the damaged elements with relative errors equal to zero; except for the damaged beams 55, 56, 57, and 58 of the second story, which were identified with a relative error of 0.1% (damage case D1). In contrast, the DSM identified five groups of damaged elements with a relative error equal to 0.1% (22–24; 37–39; 55–58; 51–54 and 46, 50). Therefore, the proposed DFM uses fewer iterations than the DSM to identify the damage; this difference can be easily observed by comparing the relative errors obtained for a given iteration value.

When one additional iteration was performed (see Table 1), both the DFM and the DSM yielded relative errors equal to zero for all damage cases studied (D1–D3), probably because both methods characterize the matrix that contains damage information in the same way (using eigenvalue decomposition and the greatest eigenvalue). The authors noticed that when the greatest eigenvalue is not used, the DFM may need an additional number of iterations, especially when the distribution of the damage is very irregular. In any case, Table 1 clearly shows that the DFM has greater sensitivity for damage detection, demonstrating excellent precision and the ability to assess damage in buildings.

It is important to note that the objective of the data analysis presented in Table 1 was to calibrate and validate the proposed method, for which complete modal information was considered. The effect of modal truncation is another important variable to be taken into account in damage detection methods based on flexibility. In order to evaluate

Table 1: Application of the DFM to the plane frame MTSAM building.

Damage case	Damaged elements	Simulated damage	Computed DSM [26]	Relative error DSM (%)	Computed DFM	Relative error DFM (%)	Number of iterations
D1	1, 5	30	30	0	30	0	5
	7, 8, 9, 36, 40	20	20	0	20	0	5
	22, 23, 24	10	9.9	0.1	10	0	5
	37, 38, 39	20	19.9	0.1	20	0	5
	55, 56, 57, 58	25	24.9	0.1	24.9	0.1	5
D2	1, 2, 3, 4, 5	20	20	0	20	0	5
	51, 52, 53, 54	40	39.9	0.1	40	0	5
D3	46, 50	20	20.1	0.1	20	0	2
	47, 48, 49	20	20	0	20	0	2
	87, 88, 89, 90	40	40	0	40	0	2

these effects on the DFM, we used a technique taken from the literature to adjust the flexibility matrices with vibration measurements.

3. Effects of Limited Modal Information and Noise

It is well known that noise in modal measurements and errors due to modal truncation are the main variables that affect structural damage detection methods based on flexibility matrices [27–30]. For this reason, we evaluated the sensitivity of DFM when these variables were considered. Therefore, a higher number of iterations could be needed, starting from Step 8 in the DFM algorithm (Figure 2). Using a higher number of iterations our method converged in all damage cases studied. The identified damage indicators are obtained in such a way that they do not change when the number of iterations increases.

In order to evaluate the effects of limited modal information and noise we first evaluated the errors due to modal truncation; then, we developed a way to simulate the noise by perturbing flexibility matrices. Finally, considering both effects combined, we applied the DFM to the numerical model of the MTSAM building (Figure 1).

3.1. Effects of Limited Modal Information. The DFM and other reported methods of damage detection are affected by the incomplete modal information of the structure under study; therefore, the method's accuracy and damage identification ability are affected. To evaluate the errors due to modal truncation in the fit of lateral flexibility matrix of the damaged structure $[\overline{F}]_D$, the Baruch system identification method was used [31]. This method establishes that the optimal vibration mode is

$$q = [\varphi] * \left[[\varphi]^T * [M] * [\varphi] \right]^{-1/2}, \quad (11)$$

where $[\varphi]$ is the matrix of modal shapes of the system and $[M]$ is the mass matrix. According to Baruch, the condensed flexibility matrix of the damaged structure can be adjusted as

$$[\overline{F}]_D = [H] * [\overline{F} - Z] + [q] * [\omega]^{-2} * [q]^T, \quad (12)$$

where $Y = [q]^T * [q] * [M]$, $Z = [\overline{F}] * [M] * [q] * [q]^T$, $H = [I] - [Y]$, and $[\omega]^{-2}$ contain the eigenvalue.

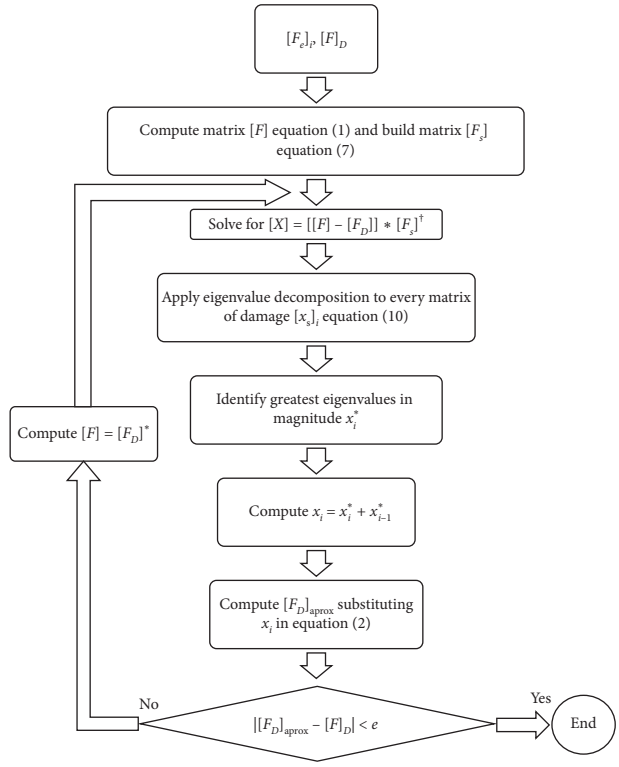

Figure 2: DFM damage detection algorithm.

We can adjust the flexibility matrix of the damaged structure $[\overline{F}]_D$ using the matrix of modal shapes $[\varphi]$ obtained from experimental measurements, equation (12). First, we need to generate a flexibility matrix $[\overline{F}]$ in a reference state; this matrix can be obtained from system identification techniques using experimental data [40], or using the geometric and mechanical characteristics of the structure [41]. Second, we need to calculate the matrix q, whose dimensions vary depending on the number of vibration modes used to adjust the flexibility matrix of the damaged structure. It should be noted that for all the damage cases studied in the present work, the mass matrix $[M]$ was assumed to be constant.

The Baruch method was used to adjust the damaged condensed flexibility matrix of the MTSAM building (Figure 1); the flexibility matrix of the building $[F]$ is 10×10,

Table 2: Damage cases studied in the MTSAM building [26].

	Damaged element	Simulated damage (% of increase in flexibility)
J1 (damaged elements of the first story)	1	40
	3	30
	5	50
J2 (damaged elements of the tenth story)	46	40
	48	30
	50	50
J3 (damaged elements of the fifth story)	21	40
	23	30
	25	50

assuming a degree of freedom per story. We analyzed the three damage cases studied by Rodríguez et al. [26] (J1 to J3) (Table 2). The flexibility matrix of the MTSAM building is assembled first, following the procedure described in Section 2. Then, the damage indicators shown in Table 2 for the three damage cases analyzed (J1–J3) are applied. Then, from the damaged flexibility matrix and the mass matrix, the frequencies and modal shapes of the MTSAM building are obtained and are then used to adjust the damaged flexibility matrix. Finally, the relative errors for each term of the main diagonal of the flexibility matrix are computed.

The first case (J1) simulates damage in three columns of the first story: elements 1, 3, and 5, with 40%, 30%, and 50% flexibility increase, respectively. The second case (J2) simulates damage in three columns of the tenth story: elements 46, 48, and 50, with 40%, 30%, and 50% flexibility increase, respectively. The third case (J3) simulates damage in three columns of the fifth story: elements 21, 23, and 25. The damage cases J1–J3 have the same damage percentages, varying only the location of the damaged story; therefore, this damage distribution allowed the evaluation of the sensitivity of the Baruch method, to adjust the flexibility matrix considering different damage positions. In Figure 3, the abscissa axis represents the number of modes used to adjust the simulated condensed flexibility matrix of the damaged structure, and the ordinate axis represents the relative errors due to modal truncation for the 10 elements of the main diagonal of the flexibility matrix.

Figures 3(a) and 3(c) show the greatest relative error values corresponding to $[\overline{F}_D]_{1,1}$ and $[\overline{F}_D]_{5,5}$, respectively. For these two damage cases (J1 and J3) the relative error values coincide with the location of the damaged story. Figure 3(b) shows the greatest relative error value $[\overline{F}_D]_{9,9}$ corresponding to a story below the one that was considered damaged (tenth story). In this model, even if we adjusted stiffness or flexibility matrices with experimental modal information using the Baruch method, the greatest relative errors are presented for the terms of the principal diagonal of the flexibility matrix corresponding to the stories where the damage occurs (cases J1 and J3) or near them (case J2). This result could be due to the fact that for both approaches the optimal vibration mode is defined in the same way (equation (11)). Despite this result, when flexibility matrices were used, lower maximum relative errors were obtained, so it is expected that lower relative errors are obtained for the same cases studied using the DFM.

Figure 3(a) (damage case J1) shows that, in order to obtain relative errors lower than 10%, four or more modes had to be used to adjust the condensed flexibility matrix. A similar behavior is observed in Figure 3(b) for case damage J2. However, for case J3, five or more modes are needed. For these damage cases studied, when flexibility matrices are used, less modal information is necessary to obtain relative errors below 10%, which is in contrast with the results obtained by Rodríguez et al. [26]. In other words, one less modal shape is needed when the flexibility matrix is used, than when we work with the stiffness matrix. In contrast to the results obtained by Rodríguez et al. [26], who needed eight or more modes to obtain the same level of relative error for cases J1 and J2, in our study all modes were required for the three damage cases studied in order to obtain errors below 2%. Therefore, to study localized damage in specific areas, it is more convenient to use the DSM.

When the first three vibration modes of the MTSAM building were used (33% of total modal shapes), the relative error values for the diagonal terms were below 10% in the damage case J1; however, the relative error value was 11.1% for the damaged story. A similar pattern was obtained for the damage case J2 (Figure 3(b)); in this case, the greatest relative error was 11.5% (using the first three vibration modes) for the story below the damaged one. In the damage case J3, all the diagonal terms were below 10%, except for $[\overline{F}_D]_{4,4}$, $[\overline{F}_D]_{5,5}$ and $[\overline{F}_D]_{6,6}$, which correspond to the damaged story, to one story below the damaged story, and to one story above the damaged story, respectively, with maximum relative errors of 9.9%, 11.4%, and 11.6%. According to these results, the relative error values ranged from 11.1% to 11.6% for all damage cases, when only the first three modes of vibration were used.

As expected, as the number of modes used to adjust the damaged flexibility matrix increased, the relative error values decreased and converged to zero when all the vibration modes were used. Nevertheless, there was no relationship between the trend of relative error values and the damaged story location. According to the results shown in Table 1, the errors due to the modal truncation effect are independent of the DFM accuracy.

3.1.1. Ten-Story Four-Bay Building Model with Limited Modal Information. It is well known that detection methods based on the flexibility matrix are affected by the limited

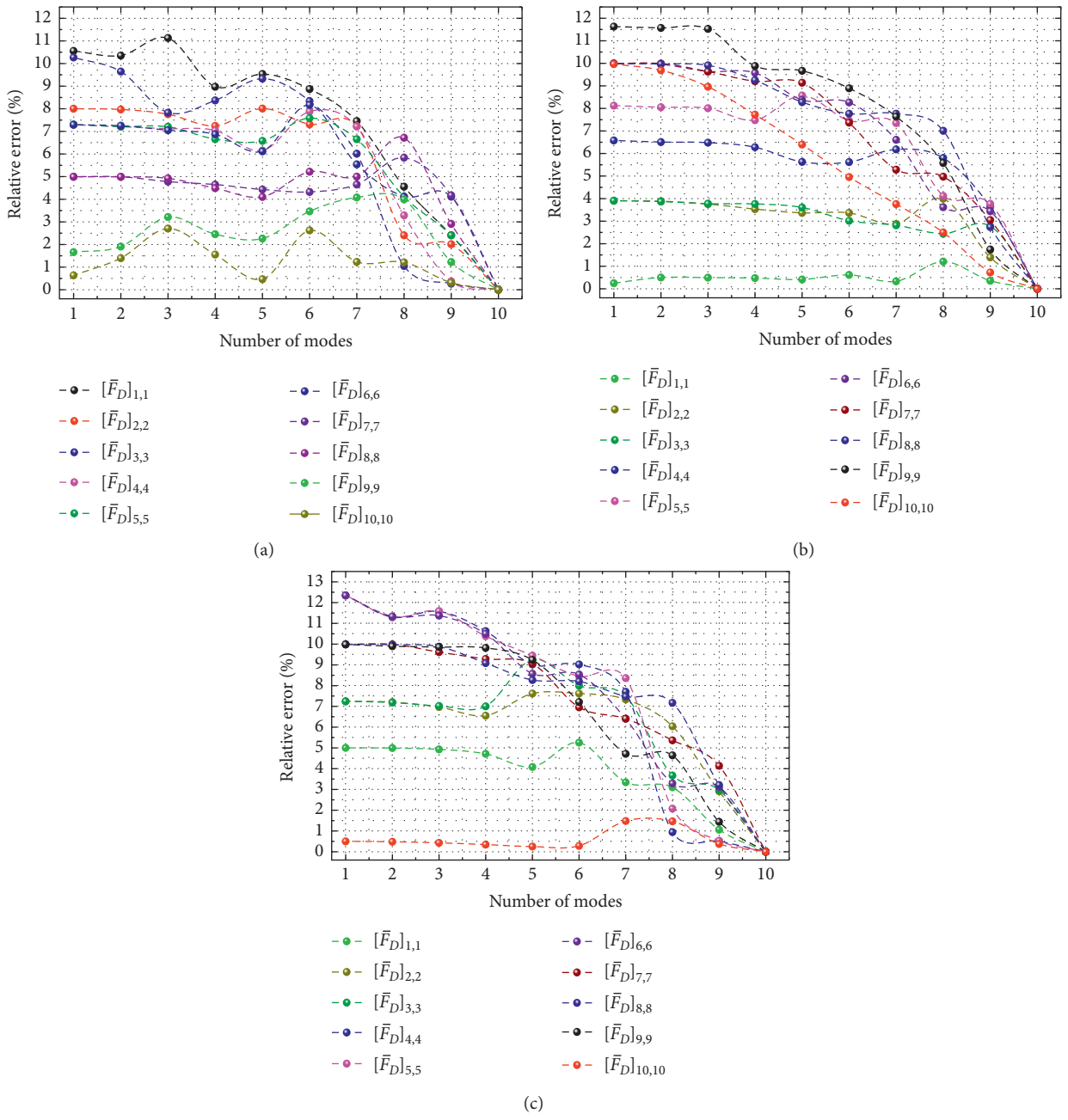

Figure 3: Relative error values between diagonal terms of simulated and computed $[F]$ considering limited modal information effects. (a) Damage case J1, (b) damage case J2, and (c) damage case J3.

modal information effects. In order to evaluate the errors derived from modal truncation in the present method (Section 2), the DFM was applied to the ten-story four-bay frame of the MTSAM building (Figure 1). First, the flexibility matrix of the damaged structure was adjusted using equation (12). Then, the calculated matrix was expanded to global coordinates, through an adjustment factor that relates the adjusted condensed flexibility matrix with modal information and the flexibility matrix of the numerical model considering all degrees of freedom.

Table 3 presents the periods for the first ten vibration modes for the MTSAM building; the dominant period was

Table 3: Periods, eigenvalues, and modal participating mass ratios of the MTSAM building.

Mode	Period (s)	Eigenvalue (rad^2/s^2)	Ratio (%)	Sum (%)
1	1.348	21.734	86.00	86.000
2	0.456	189.98	8.813	94.813
3	0.266	558.83	2.617	97.430
4	0.186	1143	1.194	98.624
5	0.143	1924.8	0.643	99.267
6	0.116	2956.9	0.294	99.561
7	0.098	4145.4	0.121	99.682
8	0.084	5572.6	0.037	99.719
9	0.076	6922	0.011	99.730
10	0.070	8052.6	0.004	99.734

1.348 s. This value is similar to the dominant periods of other buildings with similar characteristics in Mexico City, as has been reported by other authors [42]. Eigenvalues shown in Table 3 were used in equation (12) to adjust the flexibility matrix of the damaged structure. Table 3 also presents the modal participating mass ratios of the MTSAM building; the highest ratio of participating mass corresponded to the first vibration mode (86% of the total mass), and the lowest one corresponded to the tenth vibration mode (0.004% of the total mass). Therefore, the first mode has a greater contribution to the modal response of the MTSAM building and also a high contribution to damage identification (Figure 4).

To identify the damage, the expanded flexibility matrix of the damaged structure was compared with the matrix obtained from the nondamaged state using the DFM algorithm (Figure 2). The damage case J1 was studied to simulate structural damage. Figure 4 presents the relative errors calculated using the simulated damage values and the damage values calculated for three damaged elements.

The greatest relative error values were −0.20%, −0.31%, and −0.14% for elements 1, 3, and 5, respectively, which were considered damaged. These three relative error values were present when the first nine modes of vibration were used to adjust the flexibility matrix of the damaged structure. Relative errors were equal to zero when we used all 10 modes of vibration. When the first mode was used, the relative errors were equal to zero. This is convenient for practical cases studies in which only a few modal shapes can be identified. A similar trend was observed by Rodríguez et al. [26] using the DSM, possibly because both methods calculate the contribution of each structural element to damage identification using a summation of matrices. However, lower relative error values were obtained with the DFM when the modal truncation effects were considered (relative errors were below 0.5% for all damaged elements).

The relative error values for elements 1 and 5 have a similar pattern, because of the symmetry in the geometric location of these columns within the structure. Yet, the DFM presented the greatest relative error of −0.31% for element 3, while Rodríguez et al. [26] reported a relative error of −34% corresponding to element 5. According to Figure 4, for the same case studied, the DFM was less sensitive to errors derived from modal truncation than the DSM [26] because the Baruch method [31] adjusts the flexibility matrix with lower relative error values (Figure 3) than when the stiffness matrix is used.

3.2. Simulation of the Noise Effects Using Flexibility Matrices. Most of the damage detection methods reported in the literature use dynamic measurements of the structure response to nurture damage detection algorithms. These measurements include noise that affects the accuracy for identifying the damage. The DFM uses modal information (frequencies and modal shapes) to adjust the flexibility matrices, so it will be affected by noise effects. For this reason, frequencies and modal shapes were taken into account in the DFM. The objective of this section is to develop a new approach to simulate the noise effects by perturbing flexibility matrices. The effects of this perturbation mimic modal measurements affected by uncertainties in the measurements. A common practice to simulate the noise effects is to perturb modal shapes [43]. We thus used the perturbed adjusted flexibility matrices. The matrix of modal shapes disturbed by noise $[\widehat{\varphi}]$ can be calculated as

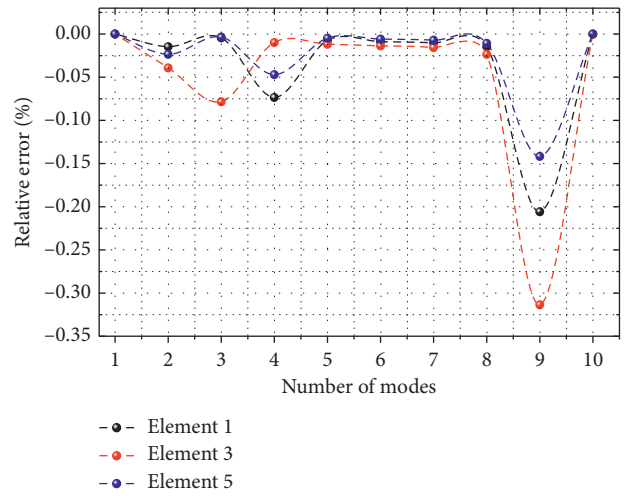

Figure 4: Magnitudes of relative error applying the DFM to the MTSAM building model with limited modal information.

$$[\widehat{\varphi}] = [\varphi] * \left(1 + \frac{N}{100} * R\right), \tag{13}$$

where N is a specific noise level (in percentage) and R is a random number with zero mean and unit variance. Equation (13) has the following form:

$$[\widehat{\varphi}] = [\varphi] * c, \tag{14}$$

where $c = 1 + (N)/(100) * R$. Substituting equation (14) into equation (11), in the optimal mode defined in Section 3.1, the perturbed optimal modal shape $[\widehat{q}]$ is

$$\begin{aligned}[\widehat{q}] &= [\varphi]c * \left\{\left[[\varphi c]^T * [M] * [\varphi c]\right]\right\}^{-1/2} \\ &= [\varphi] * \left\{\left[[\varphi]^T * [M] * [\varphi]\right]\right\}^{-1/2} = [q].\end{aligned} \tag{15}$$

Equation (11) is obtained in such a way that modal shapes are normalized with respect to mass and flexibility. After perturbing equation (12), we get

$$[\widehat{F}] = [\widehat{H}] * \left\{[F] - [\widehat{Z}]\right\} + \widehat{q} * [\widehat{\Omega}]^{-2} * \widehat{q}^T, \tag{16}$$

where $[\widehat{\Omega}] = [\Omega] * (1 + (N)/(100) * R)$, substituting $[H]$, $[Y]$, $[Z]$ into equation (16):

$$\begin{aligned}[\widehat{F}] = [F] &- [F][M][q][q]^T - [q]^T[q][M][F] \\ &+ [q]^T[q][M][F][M][q][q]^T + [q] * [\Omega]^{-2}[q]^T.\end{aligned} \tag{17}$$

Substituting $[\varphi]^T[M][\varphi] = [I]$ into equation (11) results in $[q] = [\varphi]$; substituting it into equation (17) and simplifying we get

$$[\widehat{F}] = [\overline{F}] - [\overline{F}][M][\varphi][\varphi]^T + c * [\overline{F}][M][\varphi][\varphi]^T. \quad (18)$$

Analogously to equation (13),

$$[\widehat{F}] = [F] * \left(1 + \frac{[No]}{100} * R\right). \quad (19)$$

Equating equations (18) and (19), substituting *ci,* and solving for $[No]$,

$$[No] = N * [M] * [\varphi] * [\varphi]^T. \quad (20)$$

Finally, after substituting equation (20) into (19), the perturbed flexibility matrix by noise is

$$[\widehat{F}] = [F] * \left(1 + \frac{N * [M] * [\varphi] * [\varphi]^T}{100} * R\right). \quad (21)$$

To evaluate the noise effects on the DFM, this equation was applied to the damaged condensed flexibility matrix of the ten-story four-bay building model (Figure 1). N ranged from 0 to 30% to simulate the noise effects in the system flexibility matrix.

Figure 5 shows the relative error values between $[F]$ and $[\widehat{F}]$ for each term of the main diagonal (i, i). After varying the noise levels from 0% to 30%, a similar trend for all terms studied was observed. When the noise percentage was zero, the relative error for all main diagonal terms was null, and increasing the specific noise level N increased the relative error values. This effect is expected since the random value R is applied to all components of the flexibility matrix perturbed with noise. Rodríguez et al. [26] obtained a similar trend; however, the greatest relative error value reported by them was approximately 35% for the element (10, 10), and the value obtained with this approach was 6% (Figure 5). Therefore, the methodology presented in this section demonstrated lower error levels for the same perturbation indices N after perturbation of the flexibility matrices.

It can also be observed that the greatest relative error values (10, 10) correspond to the upper story and that the relative error decreases as the stories decrease. In general, the relative error values were below 10% for all the terms of the main diagonal. Figure 5 shows that the relative error values between the terms of the main diagonal of the perturbed and unperturbed flexibility matrix are lower than 4% for noise levels (N) lower than 25%, and lower than 3% for noise levels (N) lower than 12%. We thus verified that the specific noise levels perturb flexibility matrices. Consequently, using these perturbed matrices will produce damage detection errors depending on the noise level. Yet, according to the results of the previous section, this is not a problem of the DFM (Figure 4). Nevertheless, a sensitivity study considering noise effects for different structures might be necessary to generalize these results.

4. Ten-Story Four-Bay Frame Building Model with Modal Measurements and Noise

In order to evaluate the ability of DFM for detecting damage in a more realistic way, a linear beam model was implemented in SAP2000 software of the MTSAM building frame

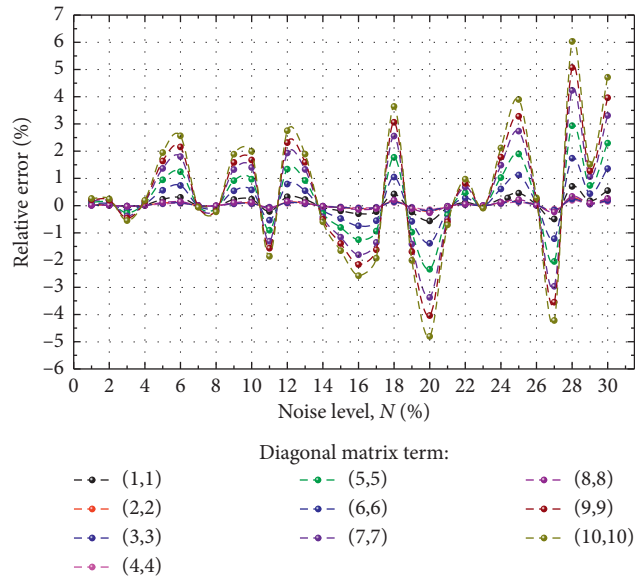

Figure 5: Relative error values between diagonal terms (i, i) of $[F]$ and $[\widehat{F}]$.

(Figure 1). This model was excited with the acceleration record of the Mexico earthquake on September 19, 1985. This earthquake was of 8.0 magnitude of moment, and the peak acceleration for the MTSAM station in the East-West direction was of 168 gals with a dominant period of 2.0 s for this particular site [44].

From the accelerations records of the stories of the MTSAM building, the frequencies and modal shapes were obtained using a signal analysis technique called Frequency Domain Decomposition (FDD), developed by Brincker et al. [45]. Figure 6 shows the variation of the singular values of the spectral density matrix of the accelerations of the 10 stories of the MTSAM building. The greatest peaks correspond to the principal frequencies of vibration, considering one degree of freedom per story. Table 4 summarizes the modal frequencies identified.

In Figure 6, the peak values of spectral density correspond to the upper story. Only the acceleration record of this story was needed to identify the principal modal frequencies of the building. A practical way to validate the modal frequencies identified is through the expression reported by Muriá and Gonzales [42] that estimates the first natural period of vibration for representative buildings in Mexico City. This expression indicates that we must divide the number of stories by 10 to obtain the natural period in seconds. One second was obtained for the MTSAM building studied, which corresponded to one hertz. This value was close to the first identified frequency in Table 4.

The modal shapes of the MTSAM building are plotted in Figure 7; they were obtained using FDD and normalized with respect to the upper story. Although a linear model in SAP2000 was used, frequencies and modal shapes were measured using recorded accelerations of the MTSAM building stories; this is in contrast with results presented in Section 3.1.1, where eigenvalue decomposition was used (Figure 4). Therefore, the DFM sensitivity for damage

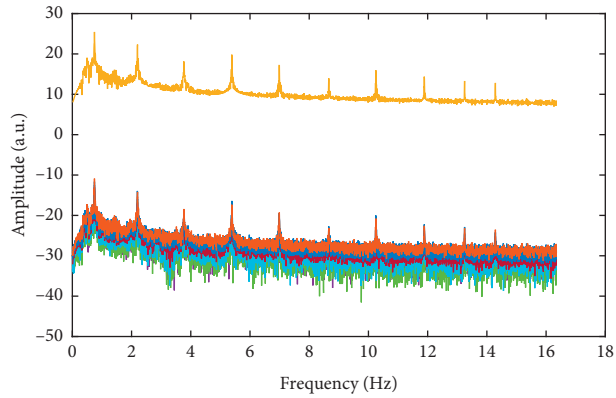

Figure 6: Variation of singular values of the spectral density matrix of the MTSAM frame building.

Table 4: Modal frequencies identified from acceleration records.

Identified mode no.	Frequency (Hz)
1	0.74
2	2.19
3	3.75
4	5.37
5	6.98
6	8.65
7	10.24
8	11.88
9	13.24
10	14.27

localization depends on the signal processing technique. However, in engineering terms, the type of mode normalization does not affect the DFM considerably (Figure 8).

Figure 8 shows the magnitude of relative error of damage values obtained by applying the DFM to the MTSAM building model with modal information measured from acceleration records. The greatest damage value was −34.81% and corresponded to element 3. When the first nine modes were used to adjust the flexibility matrices, the maximum relative errors were obtained for all damaged elements, except for element 1. However, for practical cases, it will be sufficient to use only the information of the first mode, for which relative errors below 2% were obtained. In other words, the DFM minimizes errors due to modal truncation, when it uses the first seven vibration modes of the structure. As expected, based on the results shown in Figure 3, when all modes were used, the relative error values were lowest. Note also that some values close to zero in Figure 4 increased considerably in Figure 8, due to the sensitivity of the FDD technique, and not to a defect of the DFM itself, as was already demonstrated in Table 1.

In general, as shown in Figures 4 and 8, when the first 4 or 5 vibration modes were used to adjust the flexibility matrices, lower levels of relative errors were obtained than when higher modes were used (except when all modes were used). Lower modes may have a greater contribution to the adjustment of the flexibilities matrices, as reported [46, 47]. The advantage of DFM with respect to other detection methods based on flexibility matrices is that it minimizes the adverse effect of modal truncation, even when it was applied in a more realistic scenario in a numerical model of a ten-story four-bay building. The DFM demonstrated its ability to identify the damage, minimizing errors due to modal truncation.

In addition to the effects of limited modal information, the noise effect was taken into consideration to assess the damage to the ten-story four-bay frame model (Figure 1). A specific noise level of $N = 3\%$ was used in equation (21) and the number of previously measured modes varied from 1 to 10, using equation (12). Figure 9 shows the relative error values of damage obtained after applying the DFM when simultaneously considering the noise effects and limited modal information measured. We found that the DFM was very sensitive to the noise effects. For example, when the first mode was used to adjust the flexibility matrix of the structure, error magnitudes below −35% were obtained for all the damaged elements. It is also observed that the greatest relative error value corresponds to element 1 with −194.5% of error. Figure 8 corresponds to element 3 with an error magnitude of −34.81%. This increment is due to the noise effect (Figure 9), and not to a defect of the DFM (Figure 8). The DFM thus shows excellent accuracy to assess damage when the noise effects are not included and when complete modal information is used (Table 1).

It is difficult to establish a relationship between the damage location and the optimal number of modes needed to identify the damage with error values below a specific level. In other words, we cannot establish the necessary number of modes of vibration beforehand to detect damage with a maximum value of relative error. However, for the case studied here, the lowest relative error values were obtained when the first mode was used for the three damaged simulated elements; this was achieved using theoretical modes (Figure 4), using modes measured from acceleration records (Figure 8), even considering noise effects (Figure 9). An explanation of why in these three scenarios the first mode of vibration presented low values of relative error is that the first mode provides most of the information for damage detection (Table 3). In other words, the modal participation mass ratio of the first mode is higher than the other ones, as occurs in many buildings with regular mass and flexibility distribution in height. It may be

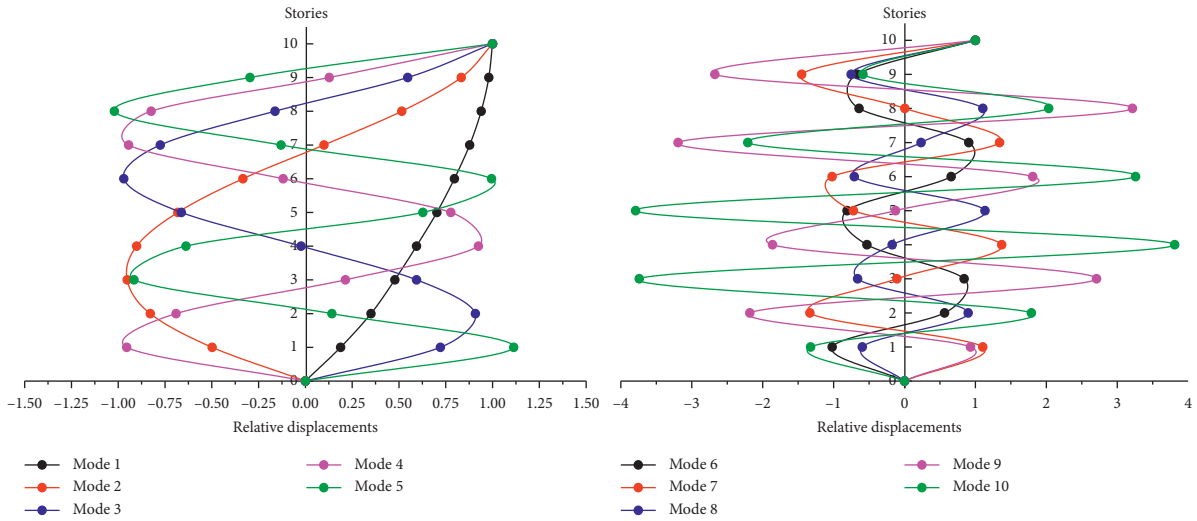

Figure 7: Modal shapes of the MTSAM frame building.

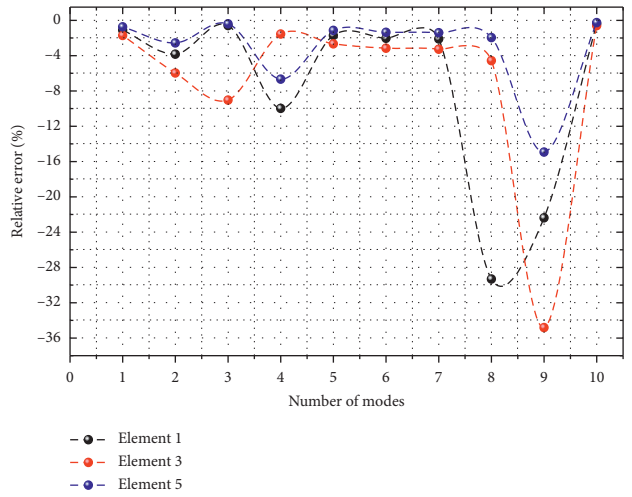

Figure 8: Relative error values applying the DFM to the MTSAM building model with modal information measurements.

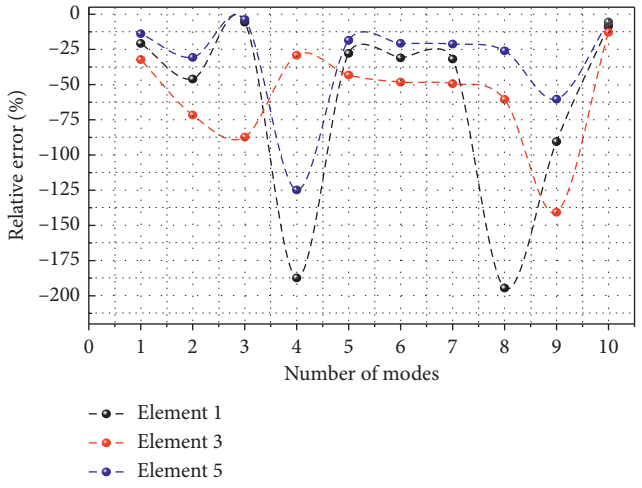

Figure 9: Relative error values obtained after applying the DFM to the MTSAM building model with modal information measurements and noise effects $N = 3\%$.

necessary to conduct sensitivity studies for damage identification, taking into account models with irregular mass and flexibility distribution. In this study, we noticed that, for structures with regular mass and flexibility distribution in height, the DFM is more sensitive for the identification of damaged elements that are relatively close to each other.

5. Conclusions

The DFM uses a new approach to assemble the damaged flexibility matrix of a frame building; through an iterative process (involving calculations of eigen parameters) the DFM identifies the flexibility increase for each structural element of a ten-story and four-bay frame building. In contrast to existing methods based on flexibility matrices, DFM minimizes the adverse effects of modal truncation, obtaining relative error magnitudes below 0.5%, when complete modal information is available.

DFM can identify structural damage with sufficient precision using only the first mode of vibration or multiple vibration modes. The DFM demonstrated excellent accuracy to assess damage cases with irregular distribution when all modal parameters are used and when noise levels are zero. The DFM was more accurate than the DSM to detect damage at the same number of iterations.

The DFM is also a new approach to simulate the noise effect perturbing flexibility matrices and can be used to develop more realistic damage identification methods without the need to modify the detection algorithms.

DFM was very sensitive to noise effects. For a specific noise level of 3% and considering modal information measured from acceleration records, the DFM identified damage with the greatest relative error value of 194.5% for element 1, and lowest value of 5.6% for the damage case J1, when the first three vibration modes were used. However, in practical cases, it would be sufficient to use the first four modes to identify the damage using the DFM. This is convenient because only a limited number of modes can be identified in realistic cases.

In addition to errors due to modal truncation and to noise effects, a source of error in the DFM was the system identification technique, through which signals were processed. Despite these sources of errors, the DFM located and assessed the damage of structural elements. Damage detection errors were mainly caused by the simulated noise and not by the method itself.

Currently, the authors are working on assessing the sensitivity of the DFM for damage detection when it is fed with other system identification techniques, as well as on developing a relationship between flexibility increase and physical damage of structural elements.

Appendix

A. Global Flexibility Matrix Assembly

We can express the total displacement D_T of a plane frame structure of N degrees of freedom as the contribution of the individual displacements of its structural elements D_i:

$$D_T = D_1 + D_2 + D_3 + \cdots + D_n, \tag{A.1}$$

where n is the total number of elements and the size of the matrices D_i is $N \times N$. According to the flexibility matrix definition, we can express equation (A.1) as

$$F_T * Q = F_1 * Q + F_2 * Q + F_3 * Q + \cdots + F_n * Q, \tag{A.2}$$

where F_T is the global flexibility matrix with the order $N \times N$. F_i are the flexibility matrices of its elements and have the following form:

$$F_i = \begin{bmatrix} \frac{L}{3EI} & -\frac{L}{6EI} \\ -\frac{L}{6EI} & \frac{L}{3EI} \end{bmatrix}, \tag{A.3}$$

where E is the modulus of elasticity, I is the area moment of inertia, and L is the length of the beam or column. These F_i just consider the bending effect and model rigid inter-elemental connections. The boundary conditions can be modeled by restraining the freedom degrees of the supports.

Q is the load vector applied in the N degrees of freedom with the order $N \times 1$ and m is the displacement number of every structural element. The individual displacements D_i of equation (A.1) can be calculated using the following compatibility equation:

$$D_i = B_i^T * p_i, \tag{A.4}$$

where B_i^T represents the transpose of the equilibrium matrix B_i of size $m \times N$. The matrices B_i relate the generalized unit loads with the internal loads of each structural element. The matrix p_i contains the deformations. Using Hooke's law we can calculate p_i as $p_i = F_i * P_i$, where P_i are the internal loads of each structural element with a size $m \times m$. Substituting equation (A.4) and p_i into equation (A.1), we can express it as follows:

$$D_T = B_1^T * F_1 * P_1 + B_2^T * F_2 * P_2 + B_3^T * F_3 * P_3 + \cdots + B_n^T * F_n * P_n. \tag{A.5}$$

Computing the matrices P_i as $P_i = B_i * Q$, replacing this expression into equation (A.5) and comparing with equation (A.2), we get

$$F_T * Q = B_1^T * F_1 * B_1 * Q + B_2^T * F_2 * B_2 * Q + B_3^T * F_3 * B_3 * Q + \cdots + B_n^T * F_n * B_n * Q. \tag{A.6}$$

Grouping and simplifying the previous equation, we finally obtain

$$F_T = B_1^T * F_1 * B_1 + B_2^T * F_2 * B_2 + B_3^T * F_3 * B_3 + \cdots + B_n^T * F_n * B_n. \tag{A.7}$$

Expressed more compactly, this equation can be written as

$$F_T = \sum_{i=1}^{n} [B]_i^T * [F]_i * [B]_i. \tag{A.8}$$

B. Damaged Flexibility Matrix Method Algorithm

(a) From the undamaged structure, build matrix $[F_s]$, which contains information of each structural element in its base state (equation (7)).

(b) Solve $[X] = [[F] - [F]_D] [F_s]^{\dagger}$, which is composed of submatrices corresponding to every damage indicator x_i for each structural element.

(c) Break down $[X]$ into N square submatrices $[x_s]_i$ (equation (9)).

(d) Apply eigenvalue decomposition (equation (10)), to every damage submatrix $[x_s]_i$.

(e) Identify the greatest eigenvalue for every value of the main diagonal of the matrix $[\Lambda]_i$; these are called damage indicators x_i^* corresponding to each element.

(f) Calculate $x_i = x_i^* + x_{i-1}^*$, for the first iteration assuming $x_{i-1}^* = 0$.

(g) Compute $[F_D]_{\text{aprox}}$ replacing x_i from the previous step into equation (2).

(h) Calculate $e = |[F_D]_{\text{aprox}} - [F]_D|$.

(i) Repeat steps 2 to 8 until $e \cong 0$; this will occur when all damage indicators of each structural element are correctly identified. The damage detection algorithm using the DFM is presented in Figure 2.

Data Availability

The data used to support the findings of this study are available from the corresponding author upon request.

Conflicts of Interest

The authors declared that there are no conflicts of interest.

Acknowledgments

This work was economically supported by Consejo Nacional de Ciencia y Tecnología (CONACyT) and Programa Institucional de Formación de Investigadores (PIFI).

References

[1] E. Rosenblueth and R. Meli, "The 1985 Mexico earthquake," *Concrete International*, vol. 8, pp. 23–34, 1986.

[2] R. Meli and J. A. Ávila, "The Mexico earthquake of September 19, 1985-analysis of building response," *Earthquake Spectra*, vol. 5, no. 1, pp. 1–17, 1989.

[3] R. Meli, "Evaluation of performance of concrete buildings damaged by the September 19, 1985 Mexico earthquake," in *The Mexico Earthquakes—1985: Factors Involved and Lessons Learned*, pp. 308–327, ASCE, Reston, VA, USA, 1987.

[4] F. Galvis, E. Miranda, P. Heresi, H. Dávalos, and J. R. Silos, "Preliminary statistics of collapsed buildings in Mexico City in the September 19, 2017 Puebla-Morelos earthquake," Technical Report, 2017.

[5] G. Milani and M. Valente, "Comparative pushover and limit analyses on seven masonry churches damaged by the 2012 Emilia-Romagna (Italy) seismic events: possibilities of non-linear finite elements compared with pre-assigned failure mechanisms," *Engineering Failure Analysis*, vol. 47, pp. 129–161, 2015.

[6] E. García-Macías and F. Ubertini, "Seismic interferometry for earthquake-induced damage identification in historic masonry towers," *Mechanical Systems and Signal Processing*, vol. 132, pp. 380–404, 2019.

[7] G. Vasdravellis, M. Valente, and C. A. Castiglioni, "Dynamic response of composite frames with different shear connection degree," *Journal of Constructional Steel Research*, vol. 65, no. 10-11, pp. 2050–2061, 2009.

[8] M. Valente, C. A. Castiglioni, and A. Kanyilmaz, "Numerical investigations of repairable dissipative bolted fuses for earthquake resistant composite steel frames," *Engineering Structures*, vol. 131, pp. 275–292, 2017.

[9] N. Cavalagli, G. Comanducci, and F. Ubertini, "Earthquake-induced damage detection in a monumental masonry bell-tower using long-term dynamic monitoring data," *Journal of Earthquake Engineering*, vol. 22, no. 1, pp. 96–119, 2018.

[10] M. Valente and G. Milani, "Earthquake-induced damage assessment and partial failure mechanisms of an Italian Medieval castle," *Engineering Failure Analysis*, vol. 99, pp. 292–309, 2019.

[11] R. Rodríguez-rocha, F. J. Rivero-Angeles, and E. Gómez-ramírez, "Application of the baseline stiffness method for damage detection of an RC building without baseline modal parameters utilizing the independent component analysis for modal extraction," *International Journal of Structural Stability and Dynamics*, vol. 13, no. 3, Article ID 1250074, 2013.

[12] J. N. Yang and S. Lin, "Identification of parametric variations of structures based on least squares estimation and adaptive tracking technique," *Journal of Engineering Mechanics*, vol. 131, no. 3, pp. 290–298, 2005.

[13] H.-F. Lam and T. Yin, "Dynamic reduction-based structural damage detection of transmission towers: practical issues and experimental verification," *Engineering Structures*, vol. 33, no. 5, pp. 1459–1478, 2011.

[14] A. Maghsoodi, A. Ghadami, and H. R. Mirdamadi, "Multiple-crack damage detection in multi-step beams by a novel local flexibility-based damage index," *Journal of Sound and Vibration*, vol. 332, no. 2, pp. 294–305, 2013.

[15] W. M. Ostachowicz and M. Krawczuk, "Analysis of the effect of cracks on the natural frequencies of a cantilever beam," *Journal of Sound and Vibration*, vol. 150, no. 2, pp. 191–201, 1991.

[16] Z. Y. Shi, S. S. Law, and L. M. Zhang, "Structural damage detection from modal strain energy change," *Journal of Engineering Mechanics*, vol. 126, no. 12, pp. 1216–1223, 2000.

[17] S. Wu, J. Zhou, S. Rui, and Q. Fei, "Reformulation of elemental modal strain energy method based on strain modes for structural damage detection," *Advances in Structural Engineering*, vol. 20, no. 6, pp. 896–905, 2017.

[18] W. Fan and P. Qiao, "Vibration-based damage identification methods: a review and comparative study," *Structural Health Monitoring*, vol. 10, pp. 83–111, 2011.

[19] M. Kouhdaragh, "Experimental investigation of damage detection in beam using dynamic excitation system," *Civil Engineering Journal*, vol. 3, no. 10, pp. 920–928, 2017.

[20] S. W. Doebling, C. R. Farrar, and M. B. Prime, "A summary review of vibration-based damage identification methods," *The Shock and Vibration Digest*, vol. 30, no. 2, pp. 91–105, 1998.

[21] H. P. Zhu, J. Yu, and J. B. Zhang, "A summary review and advantages of vibration-based damage identification methods in structural health monitoring," *Gongcheng Lixue/Engineering Mechanics*, vol. 28, pp. 1–11+7, 2011.

[22] M. Maalej, C. Y. Chhoa, and S. T. Quek, "Effect of cracking, corrosion and repair on the frequency response of RC beams," *Construction and Building Materials*, vol. 24, no. 5, pp. 719–731, 2010.

[23] O. S. Salawu, "Detection of structural damage through changes in frequency: a review," *Engineering Structures*, vol. 19, no. 9, pp. 718–723, 1997.

[24] O. S. Salawu and C. Williams, "Bridge assessment using forced-vibration testing," *Journal of Structural Engineering*, vol. 121, no. 2, pp. 161–173, 1995.

[25] Z. A. Jassim, N. N. Ali, F. Mustapha, and N. A. Abdul Jalil, "A review on the vibration analysis for a damage occurrence of a cantilever beam," *Engineering Failure Analysis*, vol. 31, pp. 442–461, 2013.

[26] R. Rodríguez, J. Alberto Escobar, and R. Gómez, "Damage location and assessment along structural elements using damage submatrices," *Engineering Structures*, vol. 31, no. 2, pp. 475–486, 2009.

[27] J. Li, B. Wu, Q. C. Zeng, and C. W. Lim, "A generalized flexibility matrix based approach for structural damage detection," *Journal of Sound and Vibration*, vol. 329, no. 22, pp. 4583–4587, 2010.

[28] S. Weng, H.-P. Zhu, Y. Xia, and L. Mao, "Damage detection using the eigenparameter decomposition of substructural flexibility matrix," *Mechanical Systems and Signal Processing*, vol. 34, no. 1-2, pp. 19–38, 2013.

[29] L. Katebi, M. Tehranizadeh, and N. Mohammadgholibeyki, "A generalized flexibility matrix-based model updating method for damage detection of plane truss and frame structures," *Journal of Civil Structural Health Monitoring*, vol. 8, no. 2, pp. 301–314, 2018.

[30] G. Bernagozzi, S. Mukhopadhyay, R. Betti, L. Landi, and P. P. Diotallevi, "Output-only damage detection in buildings using proportional modal flexibility-based deflections in unknown mass scenarios," *Engineering Structures*, vol. 167, pp. 549–566, 2018.

[31] M. Baruch, "Optimization procedure to correct stiffness and flexibility matrices using vibration tests," *AIAA Journal*, vol. 16, no. 11, pp. 1208–1210, 1978.

[32] J. Avila and R. Meli, *Análisis de la Respuesta de Edificios Típicos Ante el Sismo del 19 de Septiembre de 1985*, Informe Interno, Instituto de Ingeniería, UNAM, Mexico City, México, 1987.

[33] J. A. Escobar, J. J. Sosa, and R. Gómez, "Structural damage detection using the transformation matrix," *Computers and Structures*, vol. 83, no. 4-5, pp. 357–368, 2005.

[34] R. Rodríguez, J. A. Escobar, and R. Gómez, "The baseline stiffness method for damage detection in buildings without baseline modal parameters," *Journal of Earthquake Engineering*, vol. 15, no. 3, pp. 433–448, 2011.

[35] NTCS-04, *Normas Técnicas Complementarias Para Diseño por Sismo, Reglamento de Construcciones para el Distrito Federal*, Gaceta Oficial del Distrito Federal, Mexico City, Mexico, 2004.

[36] J. A. Escobar, J. J. Sosa, and R. Gómez, "Damage detection in framed buildings," *Canadian Journal of Civil Engineering*, vol. 28, no. 1, pp. 35–47, 2001.

[37] A. Ben-Israel and T. N. Greville, *Generalized Inverses: Theory and Applications*, Springer Science & Business Media, Berlin, Germany, 2003.

[38] R. Rodríguez, J. A. Escobar, and R. Gómez, "Damage detection in instrumented structures without baseline modal parameters," *Engineering Structures*, vol. 32, no. 6, pp. 1715–1722, 2010.

[39] L. Yu, L. Cheng, L. H. Yam, and Y. J. Yan, "Application of eigenvalue perturbation theory for detecting small structural damage using dynamic responses," *Composite Structures*, vol. 78, no. 3, pp. 402–409, 2007.

[40] A. K. Pandey and M. Biswas, "Damage detection in structures using changes in flexibility," *Journal of Sound and Vibration*, vol. 169, no. 1, pp. 3–17, 1994.

[41] M. B. Fuchs, *Structures and Their Analysis*, Springer, Berlin, Germany, 2016.

[42] D. Muriá and R. González, "Propiedades dinámicas de edificios de la cuidad de México," *Revista de Ingeniería Sísmica*, vol. 51, pp. 25–45, 1995.

[43] H. Sohn and K. H. Law, "A Bayesian probabilistic approach for structure damage detection," *Earthquake Engineering and Structural Dynamics*, vol. 26, no. 12, pp. 1259–1281, 1997.

[44] W. C. Stone, F. Y. Yokel, M. Celebi, T. Hanks, and E. V. Leyendecker, *Engineering Aspects of the September 19, 1985 Mexico Earthquake (NBS BSS 165)*, NIST, Gaithersburg, MD, USA, 1987.

[45] R. Brincker, L. Zhang, and P. Andersen, "Modal identification from ambient responses using frequency domain decomposition," in *Proceedings of the 18th International Modal Analysis Conference (IMAC)*, San Antonio, TX, USA, 2000.

[46] W.-J. Yan and W.-X. Ren, "Closed-form modal flexibility sensitivity and its application to structural damage detection without modal truncation error," *Journal of Vibration and Control*, vol. 20, no. 12, pp. 1816–1830, 2014.

[47] D. Wu and S. S. Law, "Model error correction from truncated modal flexibility sensitivity and generic parameters: Part I-simulation," *Mechanical Systems and Signal Processing*, vol. 18, no. 6, pp. 1381–1399, 2004.